

Calculation of Electric and Magnetic Field Safety Limits Under UHV AC Transmission Lines

Manash Jyoti Baishya
Dept. of Electrical Engineering
IIT Kharagpur
Kharagpur, India
Email: manashiitkgp@gmail.com

Dr. N.K. Kishore
Dept. of Electrical Engineering
IIT Kharagpur
Kharagpur, India
Email: kishor@ee.iitkgp.ernet.in

Dr. Satyajit Bhuyan
Dept. of Electrical Engineering
Assam Engineering College
Guwahati, India
Email: satyajeeetbhuyan@yahoo.co.in

Abstract - With the ever burgeoning population rate and rapid industrialisation, the demand for power has increased manifold. Ultra High Voltage AC transmission is one of the measures to arrest this increasing energy demands. This paper evaluates the safety limits for electric and magnetic fields generated around the UHV AC transmission lines. Shielding methods are also evaluated to reduce the electric field at ground level. Moreover surface current density for human beings has also been calculated.

Keywords—Electric Field; Magnetic Field; Safety Limits.

I. INTRODUCTION

Because of the manifold increase in use of electric power in modern society, the level of exposure of biological systems to electromagnetic fields have increased by several orders of magnitude in the recent past. It is important to evaluate possible interactions between the man made electromagnetic environment with humans and such interactions will be detrimental to what extent.

As per ICNIRP (International Commission on Non - Ionizing Radiation Protection), the safety limits for human beings are 5 kV/m (rms) for the electric field and 100 μ T (rms) for the magnetic field [1]. Electric Field around the transmission lines needs to be analysed for different configurations and at various heights. An efficient method to reduce the field consists of using grounded shield wires under transmission lines [2]. Shield wires of single, double and triple configuration have been used for the analysis [3],[4]. Safety limit violations of magnetic fields for various transmission line configurations, at various Surge Impedance Loading (SIL) levels is necessary to set our safety level for different conditions. So in this work the calculations have been carried out for 30% SIL, 50% SIL, 100% SIL and 110% SIL. Considering the human body to be a cylindrical structure with cylinders of different radii representing the different body parts, the surface current density calculated on a cylindrical structure, representing a body part of radius 'r' and electrical conductivity ' σ ' is related to the flux density at a frequency 'f' as follows:[5]

$$J_{rms} = \pi f r B_{rms} \sigma \text{ A/m}^2 \quad (1)$$

978-1-4799-5141-3/14/\$31.00 ©2014 IEEE

where,

J_{rms} = rms value of current density,

B_{rms} = rms value of flux density in Tesla,

σ = electrical conductivity of the tissue
= 0.2 S/m [5]

Surface current density safety limit: A human being is in danger if the surface current density over his body exceeds 1 mA/m² [6]. Though minor biological effects are reported in the range of 1-10 mA/m², but experts predict that long term exposure even at this level may prove fatal. Beyond 10 mA/m², it leads to more complex health hazards [6]. Calculations are carried out for bundled conductors.

II. GEOMETRIES USED FOR COMPUTATIONS

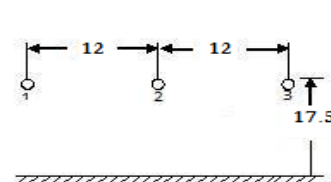


Fig.1: 1000 kV horizontal circuit line [7]

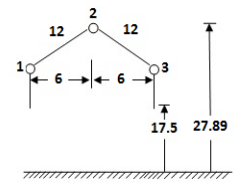


Fig.2: 1000 kV triangular circuit line

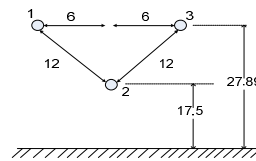


Fig.3: 1000 kV reverse triangular configuration

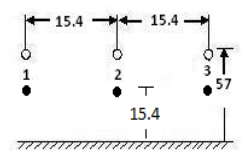


Fig. 4: 1000kV horizontal circuit line [8]

	Height of conductors (h)	Phase spacing (s)
Fig. 1	$h=17.5 \text{ m}$	$s=12 \text{ m}$
Fig. 2	$h_1=h_3=17.5 \text{ m}$, $h_2=27.89 \text{ m}$	$s=12 \text{ m}$
Fig. 3	$h_1=h_3=27.89 \text{ m}$, $h_2=17.5 \text{ m}$	$s=12 \text{ m}$
Fig. 4	$h=57 \text{ m}$, height of shield wires = 15.4 m	$s=15.4 \text{ m}$

III. CALCULATIONS [6]

A. Electric Field Calculations

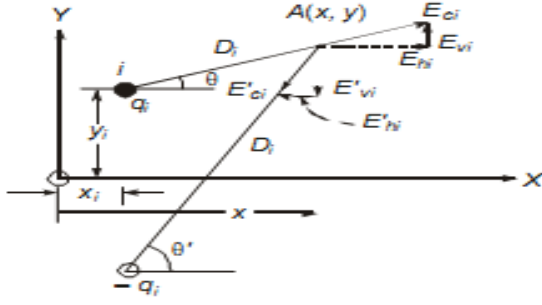


Fig. 5: Calculation of electrostatic field components near a transmission line [6]

Figure 5 shows the geometry for the calculation of the electric field at a point near a transmission line. The coordinates of the line conductors are (x_i, y_i) where $i=1$ to n , n is the number of phases of transmission. The conductor is represented by charge q_i and its image directly below is represented by $-q_i$. The coordinate of the point at which the horizontal, vertical and total electric field is found is $A(x, y)$.

For a 3-phase line constants J and K are defined and calculated as follows:

$$J_i = (x - x_i) [1/D_i^2 - 1/D'_i{}^2] \quad (2)$$

$$K_i = (y - y_i)/D_i^2 - (y + y_i)/D'_i{}^2 \quad (3)$$

where, $i = 1, 2, 3$

To check the variation of the electric field from the centre phase upto 60 m on both sides x coordinate is varied from -60 m to 60 m as it is believed over this distance electric field will be well below safe limits.

$[P]$ = $n \times n$ matrix of Maxwell's potential coefficients ;

$$M = [P]^{-1} \quad (4)$$

Using the values of matrix M , constants Kv_1 , Kv_2 and Kv_3 are calculated as follows:

$$Kv_1 = K_1 M_{11} + K_2 M_{21} + K_3 M_{31}; \quad (5)$$

$$Kv_2 = K_1 M_{12} + K_2 M_{22} + K_3 M_{32} \quad (6)$$

$$Kv_3 = K_1 M_{13} + K_2 M_{23} + K_3 M_{33} \quad (7)$$

The rms value of the total vertical component of the electric field at point $A(x, y)$ due to all three phases is:

$$Ev_n = ((Kv_1^2 + Kv_2^2 + Kv_3^2 - Kv_1 Kv_2 - Kv_2 Kv_3 - Kv_3 Kv_1)^{1/2} / 1000 / (\sqrt{3})) \quad (8)$$

Using the values of matrix M , constants Jh_1 , Jh_2 and Jh_3 are calculated as follows:

$$Jh_1 = J_1 M_{11} + J_2 M_{21} + J_3 M_{31} \quad (9)$$

$$Jh_2 = J_1 M_{12} + J_2 M_{22} + J_3 M_{32} \quad (10)$$

$$Jh_3 = J_1 M_{13} + J_2 M_{23} + J_3 M_{33} \quad (11)$$

The rms value of the total horizontal component of the electric field at point $A(x, y)$ due to all three phases is:

$$Eh_n = ((Jh_1^2 + Jh_2^2 + Jh_3^2 - Jh_1 Jh_2 - Jh_2 Jh_3 - Jh_3 Jh_1)^{1/2} / 1000 / (\sqrt{3})) \quad (12)$$

Total rms value of the electric field at point A is :

$$E = (Eh_n^2 + Ev_n^2)^{0.5} \quad (13)$$

B. Magnetic Field Calculations

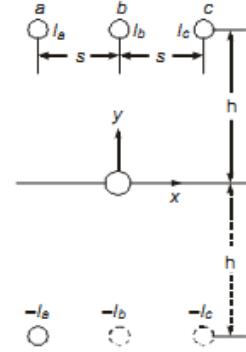


Fig. 6: Three phase overhead conductors and their images [6]

Figure 6 represents the geometry of the three phase overhead conductors and their image conductors below the ground level. The origin of the co-ordinate system is placed on the ground underneath the centre phase. Considering the arrangement shown in the above figure the horizontal components of the magnetic field is calculated as detailed below:

Constants for horizontal components k_a , k_b and k_c of the magnetic field are defined and calculated as

$$k_a = ((y+h)/((x+s)^2 + (y+h)^2)) - ((y-h)/((x+s)^2 + (y-h)^2)) \quad (14)$$

$$k_b = ((y+h)/(x^2 + (y+h)^2)) - ((y-h)/(x^2 + (y-h)^2)) \quad (15)$$

$$k_c = ((y+h)/((x-s)^2 + (y+h)^2)) - ((y-h)/((x-s)^2 + (y-h)^2)) \quad (16)$$

$$H_{ht} = (I/2\pi) (k_a^2 + k_b^2 + k_c^2 - k_a k_b - k_b k_c - k_c k_a)^{0.5} \quad (17)$$

Total flux density due to the horizontal components is:

$$B_{ht} = (4\pi \times 10^{-7}) H_{ht} \text{ T} \quad (18)$$

Constants for vertical components j_a , j_b and j_c of the magnetic field are defined and calculated as

$$j_a = ((x+s)/((x+s)^2 + (y-h)^2)) - ((x+s)/((x+s)^2 + (y+h)^2)) \quad (19)$$

$$j_b = ((x)/((x)^2 + (y-h)^2)) - ((x)/((x)^2 + (y+h)^2)) \quad (20)$$

$$j_c = ((x-s)/((x-s)^2 + (y-h)^2)) - ((x-s)/((x-s)^2 + (y+h)^2)) \quad (21)$$

$$H_{vt} = (I/2\pi) (j_a^2 + j_b^2 + j_c^2 - j_a j_b - j_b j_c - j_c j_a)^{0.5} \quad (22)$$

Total flux density due to the vertical components is:

$$B_{vt} = (4\pi \times 10^{-7}) H_{vt} \text{ T} \quad (23)$$

Total magnetic field density is :

$$B = (B_{ht}^2 + B_{vt}^2)^{0.5} \quad (24)$$

C. Electric Field Shielding Calculations [2]

Shielding Efficiency can be defined as :

$$Se = 1 - Es/Eo \quad (25)$$

where, Es = Electric field at ground level with the shield present

E_0 = Unperturbed electric field without the shield.

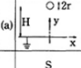
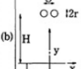
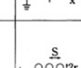
configuration	Se
(a) 	$\left(\frac{1 + \frac{y}{H}}{(\frac{H}{r})^2 + (1 + \frac{y}{H})^2} + \frac{1 - \frac{y}{H}}{(\frac{H}{r})^2 + (1 - \frac{y}{H})^2} \right) \ln \left \frac{2}{r/H} \right \quad (i)$
(b) 	$\left(\frac{1 + \frac{y}{H}}{(\frac{H}{r})^2 + (1 + \frac{y}{H})^2} + \frac{1 - \frac{y}{H}}{(\frac{H}{r})^2 + (1 - \frac{y}{H})^2} + \frac{1 + \frac{y}{H}}{(\frac{H}{r})^2 + (1 + \frac{y}{H})^2} + \frac{1 - \frac{y}{H}}{(\frac{H}{r})^2 + (1 - \frac{y}{H})^2} \right) \div \left[\ln \left \frac{2}{r/H} \right + \frac{1}{2} \ln \left(\frac{S^2 + 4}{(\frac{H}{r})^2 + (\frac{H}{r})^2} \right) \right] \quad (ii)$
(c) 	$\left(\frac{1 + \frac{y}{H}}{(\frac{H}{r})^2 + (1 + \frac{y}{H})^2} + \frac{1 - \frac{y}{H}}{(\frac{H}{r})^2 + (1 - \frac{y}{H})^2} \right) \times \frac{d-b}{ad-bc} + \left(\frac{1 + \frac{y}{H}}{(\frac{H}{r})^2 + (1 + \frac{y}{H})^2} + \frac{1 - \frac{y}{H}}{(\frac{H}{r})^2 + (1 - \frac{y}{H})^2} + \frac{1 + \frac{y}{H}}{(\frac{H}{r})^2 + (1 + \frac{y}{H})^2} + \frac{1 - \frac{y}{H}}{(\frac{H}{r})^2 + (1 - \frac{y}{H})^2} \right) \times \frac{a-c}{ad-bc}$ where $a = \ln \left \frac{2}{r/H} \right $, $b = 2c = \ln \left(\frac{S^2 + 4}{(\frac{H}{r})^2 + (\frac{H}{r})^2} \right)$, $d = a + \frac{1}{2} \ln \left(\frac{S^2 + 4}{(\frac{H}{r})^2 + (\frac{H}{r})^2} \right)$ (iii)

Table 1: Approximate expressions for shielding efficiency (Se) along with the shielding wire configuration [2]

In Table 1, the configurations of the shielding wires for transmission lines have been shown on the left side column and the right side column represents the expressions for shielding efficiency. In the table, x and y represent the coordinates of the position of the shield wires. Radius of shield wires is represented by r, H represents height of shield wires, S represents spacing between the shield wires. Equation (i) represents the shielding efficiency of only a single shield wire.

Equation (ii) represents the shielding efficiency of two shield wires.

Equation (iii) represents the shielding efficiency of three shield wires.

IV. RESULTS AND DISCUSSIONS

A. Electric Field comparison with different height of conductors.

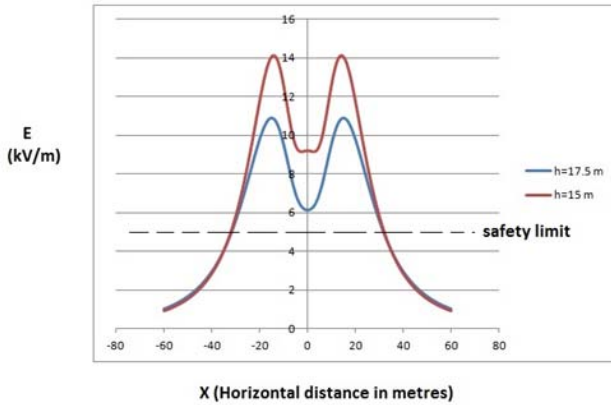


Fig.7: Electric Field comparison at 1.75 m height for different conductor heights of Fig.1

Figure 7 shows the electric field comparison for 1000 kV line configuration shown in Figure 1 with the same configuration but different heights of conductors (17.5 m & 15 m) at a height of 1.75 m from the ground level. This graph is computed to observe the electric field for a 1.75 m tall man at the uppermost plane of the body from the ground level. From the figure, it can be observed that the electric field level is more at a height of 1.75 m from the ground level for the configuration with conductors at lesser

height (i.e at 15 m) by approximately 25% directly below the conductors.

B. Electric Field for a 1.75 m tall human being under 1000 kV line in Fig.1

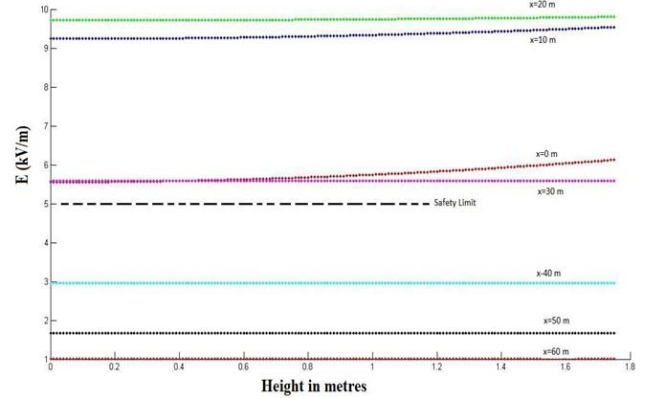


Fig.8 : Electric Field for a 1.75 m tall human being under 1000 kV line at various horizontal positions

Figure 8 shows the electric field experienced by a 1.75 m tall human being throughout his body standing at various horizontal positions $x = 0$ m to $x = 60$ m under the 1000 kV line. The electric field exposure safety limit of 5 kV/m for a human being is violated at the ground level itself for this configuration till ± 31 m on both sides of the central conductor. From the figure it can be observed that the electric field increases throughout his body as the point of interest is moved from his feet to his head. At horizontal level $x=0$ m, $x=10$ m, $x=20$ m and $x=30$ m, the safety limit is violated. At $x=40$ m, $x=50$ m and $x=60$ m electric field is within the safety limits. The peak value of electric field is experienced at the topmost point of his head.

C. Electric Field comparison for Italian 1000 kV line in Fig.1 with different phase spacing.

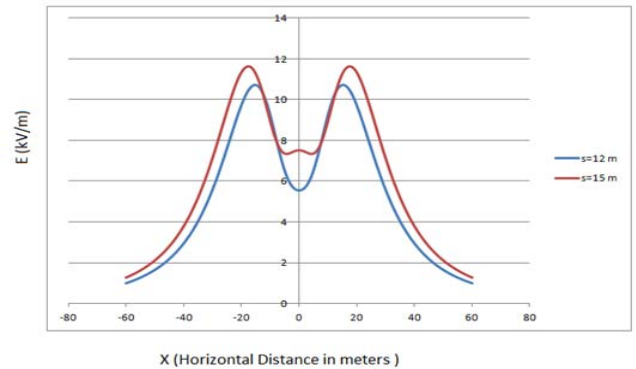


Fig. 9: Electric Field comparison at ground level for 1000 kV line with various spacing of conductors

Figure 9 shows the electric field comparison for the 1000 kV transmission line at ground level with the single circuit horizontal configuration but different phase spacing (12 m

& 15 m). From the figure, it can be seen that the electric field level increases with the increase in phase spacing. For the configuration with phase spacing of 15 m, the electric field values at the ground level is higher in comparison with the electric field values for the configuration with phase spacing of 12 m.

D. Electric Field comparison for triangular and horizontal configuration of 1000 kV line

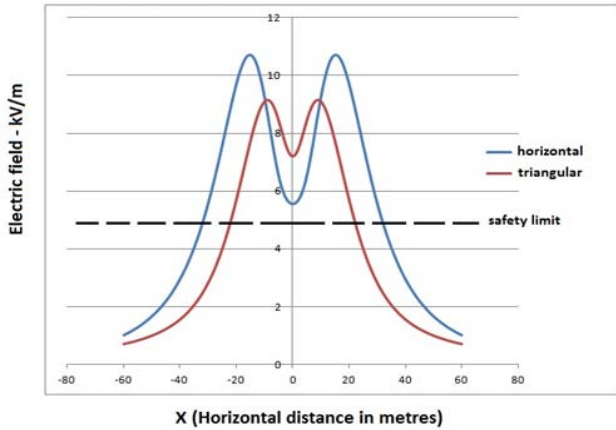


Fig.10: Electric Field comparison for horizontal (Fig.1) and triangular configuration (Fig.2) of 1000 kV line.

Figure 10 shows the comparison of electric field at ground level for the 1000 kV line with triangular and horizontal configuration. From the graph, it can be observed that the horizontal span over which the electric field safety limit of 5 kV/m for human beings is violated is wider for the horizontal configuration. For the triangular configuration, the safety limit violations take place within ± 23 m and for horizontal configuration the safety limit violations takes place ± 31 m on both sides of the origin, assuming the central conductor to be lying on the vertical axis passing through the origin.

E. Electric field comparison at ground level for 1000 kV line with triangular and reverse triangular configuration

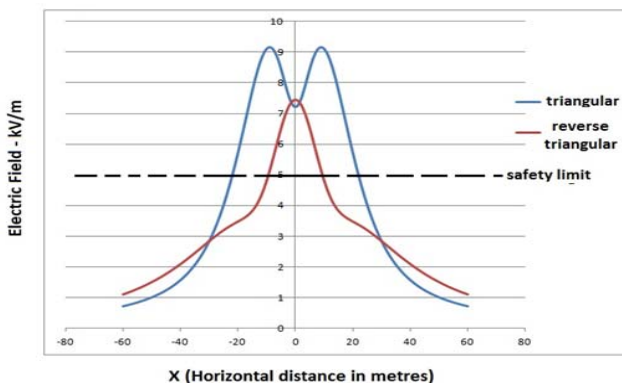


Fig.11: Electric Field comparison for triangular (Fig. 2) and reverse triangular configuration of 1000 kV line (Fig. 3)

Figure 11 shows the electric field at ground level for the 1000 kV line with triangular and reverse triangular configuration. From figure 11, it can be observed that the

electric field at the ground level is higher for the triangular configuration and the electric field values for the reverse triangular configuration are lower. It can also be observed that the electric field safety limit violations for human beings under the triangular configuration take place within ± 23 m on both sides of the origin, assuming the central conductor to be lying on the vertical axis passing through the origin. For the reverse triangular configuration, the safety limit violations take place within ± 16 m. So the reverse triangular configuration permits lesser right of way.

F. Right of Way calculations

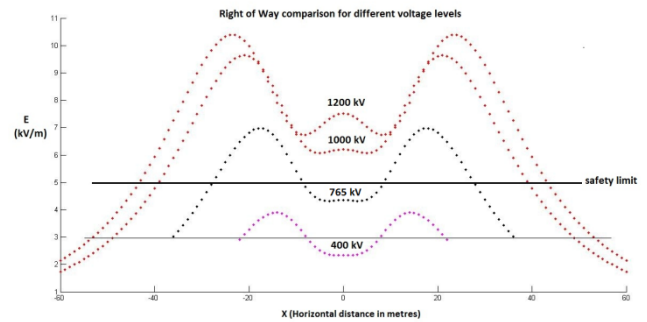


Fig.12 : ROW calculation for UHV AC lines

Estimating the right of way for a 1000 kV and 1200 kV single circuit horizontal configuration line with average values of line parameters has been carried out by comparing the electric field at 1 m height from the ground level for 400 kV and 765 kV single circuit horizontal configuration lines with average values of line parameters. Figure 12 represents the electric field at 1 m height from the ground level for 400 kV, 765 kV, 1000 kV and 1200 kV single circuit horizontal lines with average values of line parameters. The right of way for 400 kV line is 52 m and for 765 kV line it is 64 m [8]. From the graph, at $x = \pm 26$ m (52 m ROW) for 400 kV line, the electric field is 3 kV/m (rms), for 765 kV line, at $x = \pm 32$ m (64 m ROW), the electric field is around 3 kV/m (rms). For the 1000 kV line the rms value of the electric field of 3 kV/m is experienced at $x = \pm 48$ m and for the 1200 kV line it is experienced at $x = \pm 52$ m. So, by comparing the electric field values, the right of way for 1000 kV line has been calculated to be 96 m and for 1200 kV line it is 104 m.

G. Electric Field shielding calculations for Fig.4

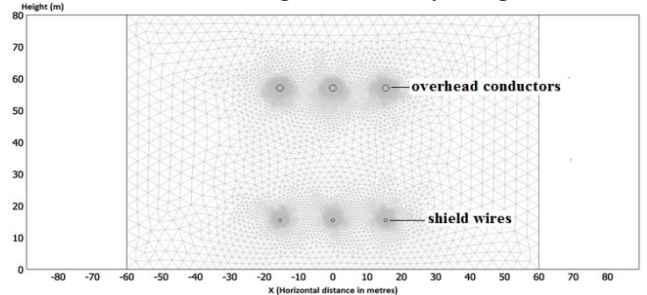


Fig.13: Geometry of overhead conductors and shield wire arrangement for 1000 kV line in Fig.4

Figure 13 presents the arrangement of conductors and shield wires for the 1000 kV line shown in figure 4. Three shield wires are placed directly below the overhead conductors at $x = -15.4$ m, $x = 0$ m, $x = 15.4$ m. The height of shield wires is 15.4 m, radius of shield wires is 10.5 mm and spacing between shield wires is 15.4 m.

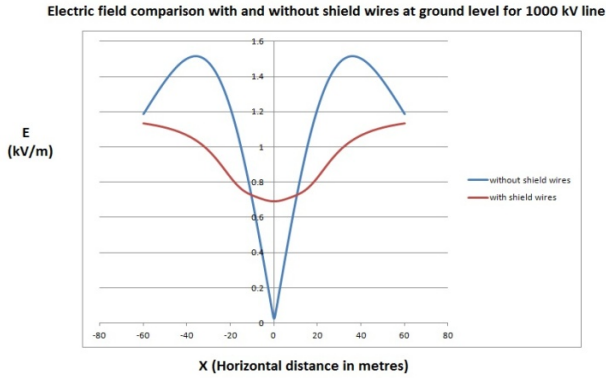


Fig.14: Electric Field at ground level with and without shield wires for 1000 kV line in Fig.4

Figure 14 shows the electric field at ground level with and without the shield wires. Initially, without the shield wires the computed electric field at ground level is higher than the electric field computed at the ground level with the presence of the shield wires. From the graph, it can be seen that the shield wires present below the outer phase overhead conductors on both the sides of the central phase conductor lying on the vertical axis passing through the origin, reduce the electric field at the ground level by approximately 21 %.

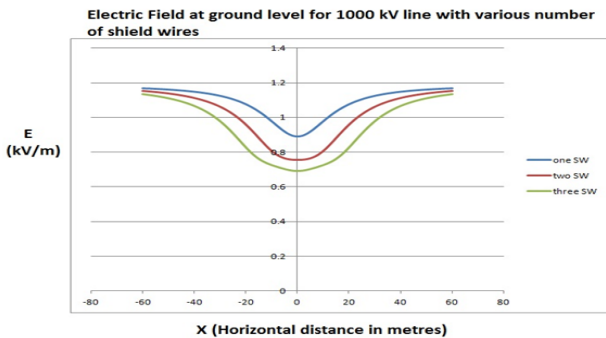


Fig.15: Electric Field at ground level with various number of shield wires for 1000 kV line in figure 4

Figure 15 shows the electric field at ground level with various number of shield wires. This figure shows the electric field at ground level due to presence of one, two and three shield wire configurations. From the figure, it is apparent that with the increase in number of shield wires the electric field at ground level is reduced further. In the figure, it is seen that the electric field at ground level is highest for single shield wire configuration and lowest for three shield wire configuration.

H. Magnetic Field Calculations at different SIL levels

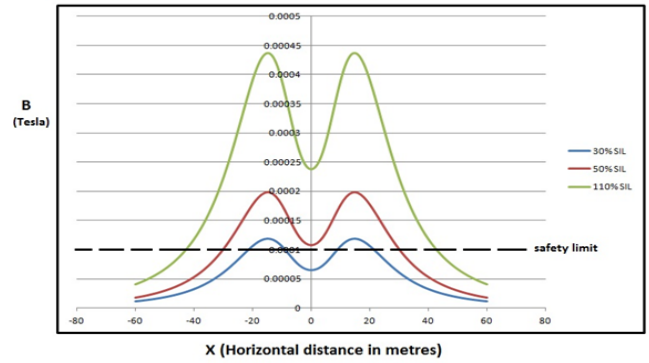


Fig.16: Magnetic field at ground level for the 1000 kV line configuration in figure 1 with various levels of SIL

Figure 16 presents the comparison of magnetic field at ground level for Italian 1000 kV line at various levels of Surge Impedance Loading. The comparisons are made for 30%, 50% and 110% SIL. From figure16, it can be seen that the horizontal span within which the magnetic field exposure safety limit for human beings is violated for the same conductor configuration increases with the increase in Surge Impedance Loading level. For 30% SIL, the safety limit violation takes place within ± 24 m, for 50% SIL violation is within ± 30 m and for 110% SIL violation is within ± 42 m. In the figure, at 30 % SIL, the safety limit violation range is minimum and at 110 % SIL, the safety limit violation range is maximum.

I. Surface Current Density calculations for a 1.75 m tall human being

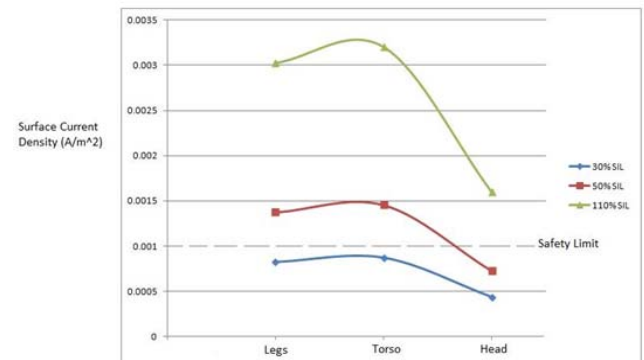


Figure 17: Peak Surface Current density for a 1.75 m tall man under the 1000 kV line in Fig.1

Figure 17 shows the peak values of the Surface Current Density for a 1.75 m tall man standing directly below the outer phase of the overhead line under the Italian 1000 kV line at various levels of SIL. The values have been plotted for legs, torso and head of the human being. From the graph, it is clear that the surface current density safety limit of 1 mA/m^2 [11] for the human being is violated at 50% SIL and 110% SIL. And the maximum value of the Surface Current Density is felt at the torso for a human being.

V. CONCLUSION

Under UHV AC Transmission Lines, activities of human beings is hazardous from various angles related to safety. The horizontal span over which the safety limit for electric and magnetic field is violated depends on the height and spacing of the overhead conductors.

The safety limit violations range is larger for horizontal conductor configuration than triangular conductor configuration. But the violation range for reverse triangular configuration is lesser compared to the other conductor configurations. However, for horizontal conductor configuration due to the use of the shielding wires below the UHV AC transmission lines, the electric field at the ground level is further reduced. The right of way for a 1000 kV line has been calculated to be around 96 m and for a 1200 kV line it has been calculated to be around 104 m. From the comparison of magnetic field of the UHV AC transmission lines, at ground level and at various levels of SIL, it is observed that the magnetic field exposure safety limit violations for human beings for the same conductor configuration increases with the increase in Surge Impedance Loading level.

For the surface current density calculation at various levels of SIL, it can be seen that the surface current density for the human being under UHV AC Transmission Lines increases with the increase in SIL. Moreover, the peak value of the surface current density for a 1.75 m tall human being can be experienced at the torso part of the human body.

ACKNOWLEDGMENT

Heartfelt gratitude and sincerest thanks to the faculties of IIT Kharagpur and the Dept. of Electrical Engineering of IIT Kharagpur for providing the best of opportunities and facilities for carrying out the research work in an organised manner.

REFERENCES

- [1] ICNIRP Guidelines, "Guidelines for limiting exposure to time-varying electric, magnetic, and electromagnetic fields, up to 300GHz", ICNIRP, 1998
- [2] Tadasa Takuma, Tadashi Kawamoto, Mitsuru Yasui, Mitsuharu Murooka and Jun Katoh, "Analysis of effect of shield wires on electrostatic induction by AC Transmission lines", IEEE Transactions on Power Apparatus and Systems, Vol. PAS-104, No. 9, pp. 2612-2618, 1985
- [3] R.M. Radwan, A.M. Mahdy, M. Abdel Salem and M.M. Samy, "Electric Field Mitigation under Extra High Voltage Power Lines", IEEE Transactions on Dielectrics and Electrical Insulation, Vol. 20, No. 1, February 2013.
- [4] D.W. Deno and J.M. Silva, "Transmission line electric field shielding by objects", IEEE Transactions on Power Delivery, Vol. PWRD - 2, No. 1, pp. 269-279, 1987.
- [5] Prof. Ahmed Hossa, DI Eldin Kamelia and Youssef Hanaa Karawia, "Investigations of induced currents in human bodies due to exposure to emf from low voltage appliances", pp. 525, Middle East Power Systems Conference 2006.
- [6] Rakosh Das Begamudre, "Extra High Voltage AC Transmission Engineering", New Age International Publishers, Third Edition, 2009.
- [7] A. Ardito, M. de Nigris, A. Giorgi, A. Pignini, A. Porrino, "The Italian 1000 kV project", International workshop on UHVAC Transmission Technology, pp. 1-11, Beijing, China, 2005.
- [8] Zhanqing Yu, Qian Li, Rong Zeng, Jinliang He, Yong Zhang, Zhizhao Li, Chijie Zhuang, Yongli Liao, "Calculation of surface electric field on UHV transmission lines under lightning stroke", Electric Power Systems Research 94 (2013) 79 – 85.
- [9] "Transmission and Distribution in India, A report", A joint initiative of World Energy Council and Power Grid Corporation of India Limited, 2012